IX. ELECTRODYNAMICS OF MEDIA

Academic Research Staff

Prof. Hermann A. Haus
Prof. Jin-Au Kong
Prof. Paul L. Penfield, Jr.
Prof. David H. Staelin
Prof. Abraham Szöke

Graduate Students

Donald L. Lee
Eni G. Njoku
Leung Tsang

RESEARCH OBJECTIVES AND SUMMARY OF RESEARCH

JSEP

1. Subsurface Probing and Communication with a Dipole Antenna

Joint Services Electronics Program (Contract DAAB07-74-C-0630)

Jin-Au Kong

In the past six months studies have been made of a horizontal electric dipole antenna laid on the surface of a stratified medium.[1-4] Employing the integral representation for the field solutions, we first used the geometrical optics approximation to calculate interference patterns as a function of distance for data interpretation, and then used the residue method to express results in terms of normal modes of the layered structure. In extending to a multilayer model, the Fast Fourier Transform (FFT) method was employed. By comparing these theoretical approaches, we have established their regions of validity, and used the results to interpret field data as well as results obtained from controlled laboratory experiments. The interpretations have been confirmed by other geophysical prospecting methods. The case of anisotropic earth was also considered.

In future investigations, we shall study sources other than horizontal electric dipoles and scattering effects. Interference patterns plotted as a function of frequency will be examined. Pulses, rather than continuous waves, will also be investigated because of their application to geophysical prospecting and subsurface communication.

References

1. L. Tsang and J. A. Kong, "Electromagnetic Fields Due to a Horizontal Electric Dipole Laid on the Surface of a Two-Layer Medium," IEEE Trans., Vol. AT-22, No. 5, pp. 709-711, September 1974.
2. J. A. Kong and L. Tsang, "Theory of Radio-Frequency Interferometry in Geophysical Subsurface Probing," Technical Report CSR-TR-74-2, Center for Space Research, M.I.T., April 1974.
3. J. A. Kong, L. Tsang, and G. Simmons, "Geophysical Subsurface Probing with Radio-Frequency Interferometry," IEEE Trans., Vol. AP-22, No. 4, pp. 616-620, July 1974.
4. L. Tsang and J. A. Kong, "Application of the Radio-Frequency Interferometry Method to Stratified Anisotropic Earth," Quarterly Progress Report No. 114, Research Laboratory of Electronics, M.I.T., July 15, 1974, pp. 87-90.

JSEP

JSEP

2. Optics of Nonisotropic Media and Optical Systems

Joint Services Electronics Program (Contract DAAB07-74-C-0630)

Jin-Au Kong

Our studies of the theorems of bianisotropic media and moving media continue.[1-4] We shall use MACSYMA[2,5] to study the optics of nonisotropic media. We plan to develop a systematic analytic approach to problems involving electromagnetic waves in nonisotropic media. The problem areas that we propose to study include guided waves and integrated optics, and optics of bianisotropic and accelerated media. We shall study mode conversion and mode coupling for the guided waves. Specifically, we shall apply the variational principle and the boundary perturbation technique to treat nonisotropic waveguides. These studies will be carried out mainly for anisotropic guides by generalizing those obtained for isotropic guides. We shall also consider macroscopic quantization of electromagnetic waves and treat rotating and linearly accelerating media.

References

1. H. A. Haus, J. A. Kong, and P. Penfield, Jr., "Comments on 'Further Remarks on the Principle of Virtue Power'," Lett. Nuovo Cimento, Vol. 10, No. 6, pp. 222-226, 8 June 1974.

2. J. A. Kong, "Analytical Studies of Electromagnetic Problems with MACSYMA," International Union of Radio Science USNC-URSI Symposium, Atlanta, Georgia, June 13, 1974, p. 82.

3. S. D. Fanton and J. A. Kong, "Scattering of TM Waves by a Surface Deformation on a Uniaxial Slab Waveguide," Optical Society of America Fall Meeting, Houston, Texas, October 15, 1974.

4. J. A. Kong, "Optics of Bianisotropic Media," Optical Society of America Spring Meeting, Washington, D. C., April 22, 1974; J. Opt. Soc. Am. 64, 1304-1308 (1974).

5. Zemen Lebne-Dengel, Eni G. Njoku, and Jin-Au Kong, "MACSYMA Studies of Waves in Uniaxial Media," Quarterly Progress Report No. 114, Research Laboratory of Electronics, M. I. T., July 15, 1974, pp. 86-87.

JSEP

3. Microwave Remote Sensing of the Earth

California Institute of Technology (Contract 953524)

Jin-Au Kong, David H. Staelin

In order to interpret the remote sensing data collected from spacecraft and satellites, we need theoretical models that are practical and useful. The effects that control emission properties of the earth include surface roughness, stratification, absorption, anisotropy, inhomogeneities, submerged scattering centers, nonuniform temperature distributions, etc. We have started to develop composite models[1] to account for these various effects. The effect of roughness on emissivity from the earth has been considered.[2] The study of a two-layer model composed of random media is now in progress. The probing depth for microwave remote sensing of ice- and snow-covered water or land has been estimated with a seminumerical approach. A summary report has been presented to URSI.[3]

In future studies we shall direct our attention toward microwave emission properties of natural surfaces, taking into account the various surface and subsurface features. Atmospheric effects will be considered, although we shall concentrate on frequencies that are least affected by atmospheric absorption. Our studies will be concentrated on developing theoretical modes for passive remote sensing. The models will be tested by comparison with observed microwave emission as a function of temperature, frequency, polarization, and viewing angles. The development of a model that is close to reality for various circumstances, and yet mathematically tractable, is our objective in this project.

References

1. J. A. Kong, "Composite Model for Microwave Remote Sensing," Quarterly Progress Report No. 114, Research Laboratory of Electronics, M. I. T., July 15, 1974, pp. 78-90.

2. L. Tsang and J. A. Kong, "Effect of Surface Roughness on Emissivity," Quarterly Progress Report No. 114, Research Laboratory of Electronics, M. I. T., July 15, 1974, pp. 75-77.

3. J. A. Kong, "Theoretical Models for Microwave Remote Sensing of Ice and Snow," URSI Specialist Meeting on Scattering and Emission from the Earth, Bern, Switzerland, September 25, 1974.

JSEP

A. STRATIFICATION FACTORS FOR THE HIGHLY CONDUCTIVE EARTH

Joint Services Electronics Program (Contract DAAB07-74-C-0630)

Jin-Au Kong, Leung Tsang

The electromagnetic fields of a dipole antenna laid on a conducting medium can be calculated from the integral

$$J = \int_{-\infty}^{\infty} dk_\rho \frac{k_\rho H_o^{(1)}(k_\rho \rho)\, e^{ik_z z}}{k_z + K k_{1z}},$$

where $H_o^{(1)}(k_\rho \rho)$ is the zero-order Hankel function of the first kind, $k_z = \left(k^2 - k_\rho^2\right)^{1/2}$, and $k_{1z} = \left(k_1^2 - k_\rho^2\right)^{1/2}$. In the case of a half-space conducting medium, $K = \epsilon_o/\epsilon_1$. The asymptotic solution to the integral as $k_\rho \rho \to \infty$ and $z/\rho \ll 1$ is

$$J = 2\frac{e^{ikr}}{r}\left[i + (\pi p_1)\, e^{-p_2}\, \text{erfc}\,(i\sqrt{p_2})\right],$$

where $p_1 = i\dfrac{k^3 \rho}{2k_1^2}$, $p_2 = p_1\left(1 + \dfrac{k_1 z}{k_o^2}\right)^2$, and erfc is the complement error function. This solution is for TM waves; for TE waves the solution is also well known.[1]

In the case of a stratified anisotropic and conducting medium, K is the stratification

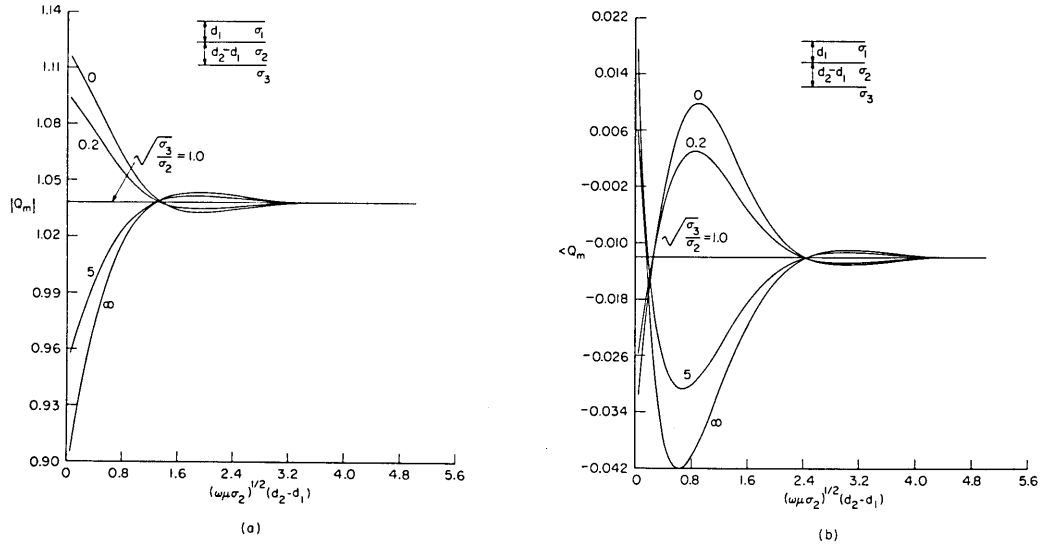

Fig. IX-1. Stratification factor of TM waves for the three-layer case: (a) magnitude; (b) phase.

JSEP

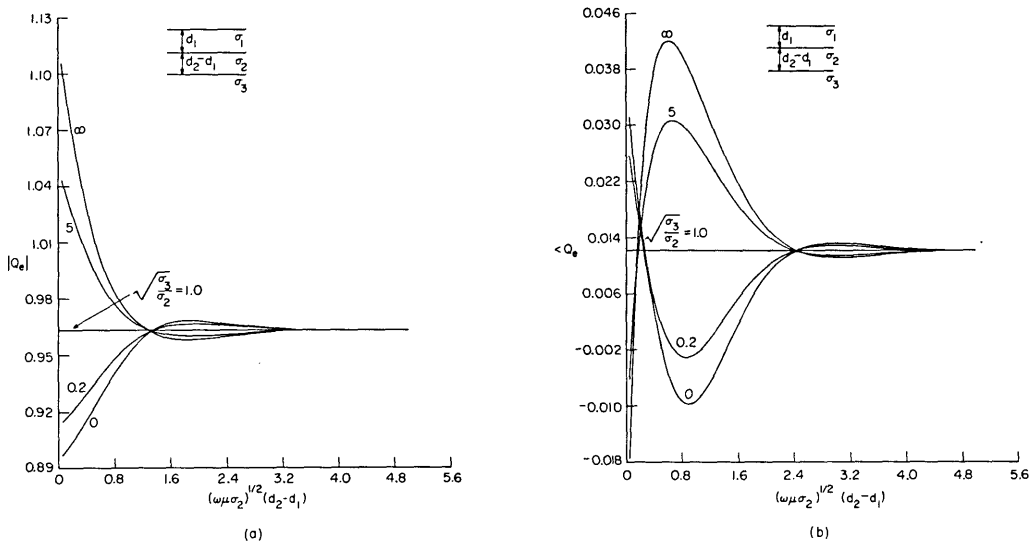

Fig. IX-2. Stratification factor of TE waves for the three-layer case: (a) magnitude; (b) phase.

factor. For TE waves $K = \epsilon/\epsilon_1\, Q^{TE}$ and for TM waves $K = \mu/\mu_1\, Q^{TM}$. For both TM and TE cases, $Q = (1-R_{n-1})/(1+R_{n-1})$, where R_{n-1} is the reflection coefficient of an n-1 layer medium.[2] Typical numerical values for Q^{TM} and Q^{TE} have been calculated for the three-layer case and both magnitudes and phases are plotted in Figs. IX-1 and IX-2. It can be seen from the curves how the conductivity and depth of the layer below influences the upper layer. These data are used to obtain field quantities of the n layer medium from the analytical half-space solutions.

References

1. J. R. Wait, "The Magnetic Dipole over the Horizontally Stratified Earth," Can. J. Phys. 29, 577-592 (1951).

2. J. A. Kong, "Electromagnetic Fields Due to Dipole Antennas over Stratified Anisotropic Media," Geophys. 37, 985-996 (1972).

B. VERTICAL ELECTRIC DIPOLE OVER A UNIAXIAL DIELECTRIC-COATED CONDUCTOR

Joint Serivces Electronics Program (Contract DAAB07-74-C-0630)

Leung Tsang, Jin-Au Kong

For a vertical hertzian electric dipole placed on the surface of a uniaxial dielectric-coated conductor (Fig. IX-3) the E_z component of the electromagnetic field on the surface is given by

JSEP

$$E_z = \int_{-\infty}^{\infty} dk_\rho \left(-\frac{I\ell}{8\pi\omega\epsilon}\right) \frac{2k_\rho^3}{k_z - ik\Delta} H_o^{(1)}(k_\rho\rho), \tag{1}$$

where

$$\Delta = \frac{a\left(ak_1^2 - k^2\right) kd}{k_1^2},$$

$H_o^{(1)}(k_\rho\rho)$ is the zero-order Hankel function of the first kind, $k_z = \left(k^2 - k_\rho^2\right)^{1/2}$, and the dielectric permittivity tensor is given by

$$\bar{\bar{\epsilon}}_1 = \begin{bmatrix} \epsilon_1 & 0 & 0 \\ 0 & \epsilon_1 & 0 \\ 0 & 0 & a\epsilon_1 \end{bmatrix}.$$

In the integral expression in (1), we have made the assumption that the thickness d of the dielectric is very small compared with a wavelength. The case of a magnetic line

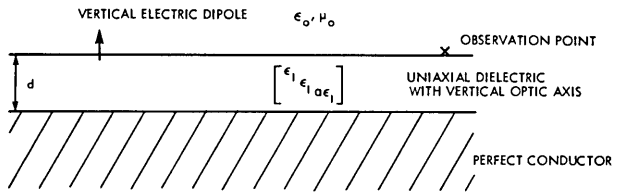

Fig. IX-3. Vertical electric dipole placed on the surface of a uniaxial dielectric-coated conductor.

source over an isotropic dielectric-coated conductor was considered by Wait.[1] The contribution to the integral in (1) is caused by a pole at $k_z = ik\Delta$, which corresponds to the excitation of the TM_0 mode, and a branch point at $k_\rho = k$ arising from k_z, which corresponds to the direct wave from the dipole. We define an effective numerical distance[2]

$$S = \frac{i\xi_o^2 k\rho}{2}, \tag{2}$$

where $\xi_o = -i\left[2\left(\sqrt{1+\Delta^2} - 1\right)\right]^{1/2}$. We use the modified saddle-point method[3] to evaluate the branch cut contribution.

JSEP

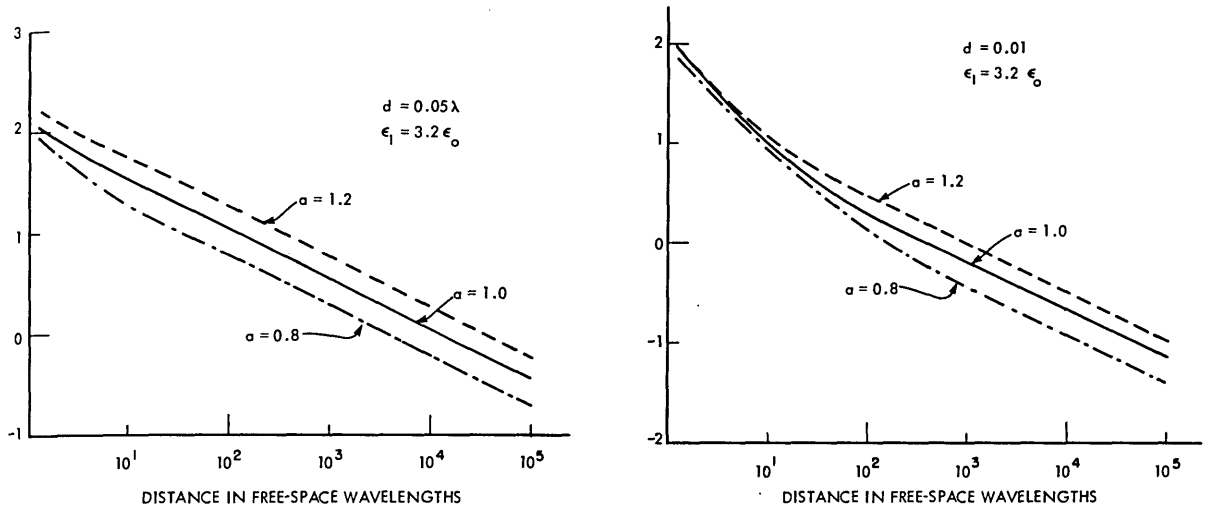

Fig. IX-4. Field amplitude as a function of distance from the dipole for the nonconductive case. (a) d = 0.05 λ. (b) d = 0.01 λ.

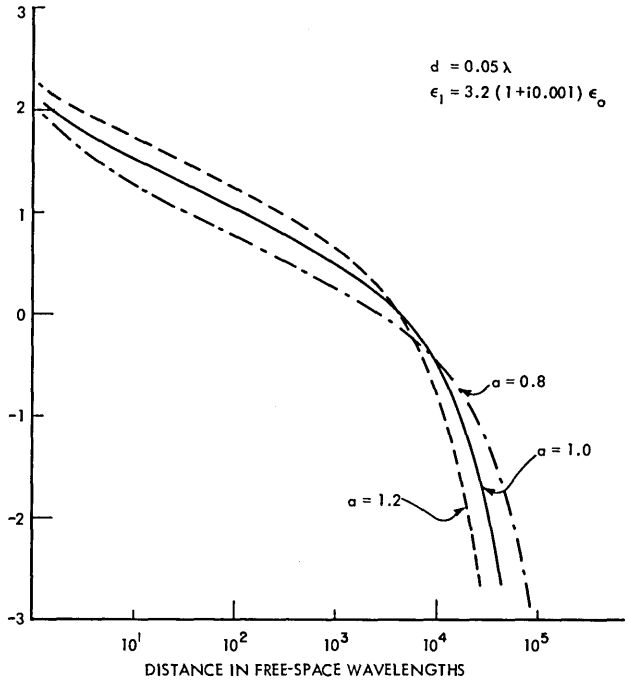

Fig. IX-5. Field amplitude as a function of distance from the dipole for the conductive case with dielectric thickness d = 0.05 λ.

JSEP

$$E_z = i\frac{I\ell}{4\pi\omega\epsilon}\frac{2k^2}{\rho}e^{ik\rho}\left[\left(\frac{k_{\rho o}}{k}\right)^{3/2}\frac{\Delta}{i\xi_o}+\frac{1}{ik\rho}\left(\frac{1}{\Delta^2}+\left(\frac{k_{\rho o}}{k}\right)^{3/2}\frac{\Delta}{i\xi_o^3}\right)\right]$$

$$+\pi\frac{I\ell}{4\pi\omega\epsilon}k_{\rho o}^2 k\Delta H_o^{(1)}(k_{\rho o}\rho)\left\{\operatorname{erfc}\left(i\sqrt{s}\right)-2\right\}, \tag{3}$$

where $k_{\rho o}$ is the location of the pole in the k_ρ plane, and erfc is the complementary error function.

For a large effective numerical distance, $|s| \gg 1$, the result in (3) reduces to that of the ordinary saddle-point method.

$$E_z = \frac{I\ell}{4\pi\omega\epsilon}\frac{2k}{\rho^2}\frac{e^{ik\rho}}{\Delta^2}-2\pi\left(\frac{I\ell}{4\pi\omega\epsilon}\right)k_{\rho o}^2 k\Delta H_o^{(1)}(k_{\rho o}\rho). \tag{4}$$

In Figs. IX-4 and IX-5 the field amplitude is plotted as a function of distance on a log-log scale for various dielectric permittivities and thicknesses. We note that in the near-field region the field is a combination of the direct wave and the guided wave, while in the far-field region, the guided wave dominates in the nonconductive case, and the direct wave dominates in the conductive case.

References

1. J. R. Wait, Electromagnetic Waves in Stratified Medium (Pergamon Press, London, 1970).
2. A. Sommerfeld, Partial Differential Equations in Physics (Academic Press, New York, 1964).
3. B. L. Van Der Waerden, "On the Method of Saddle Points," Appl. Sci. Res. B2, 33-45 (1951).

C. MODE CONVERSION WITH AN ELECTRO-OPTICAL SUBSTRATE

Joint Services Electronics Program (Contract DAAB07-74-C-0630)

Blake A. Goss, Jin-Au Kong

A study has been made of the feasibility of modulation by mode conversion in a thin-film waveguide with an electro-optical substrate. The longitudinal configuration is shown in Fig. IX-6. We assume a substrate made of a dielectric material KT_aNbO_3 that has a Curie point at 60°C and an electro-optical coefficient of 1.4×10^{-6} cm/volt. The indices of refraction are $n_e = 2.275$ and $n_o = 2.318$. A 10 volt/cm field is used. With the refractive index for the film $n = 3.34$ and the angle of incidence $\theta_i = 44°$, by a ray optical approach, the minimum modulation length is calculated to be $d = 0.376$ cm. In Fig. IX-7 the minimum modulation length is plotted against the refractive

JSEP

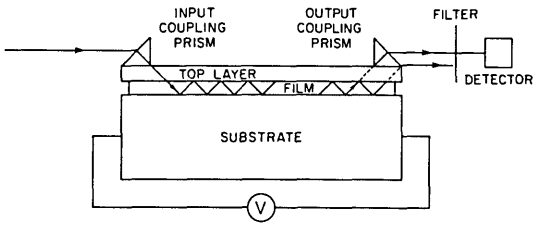

Fig. IX-6. Input coupling and detection.

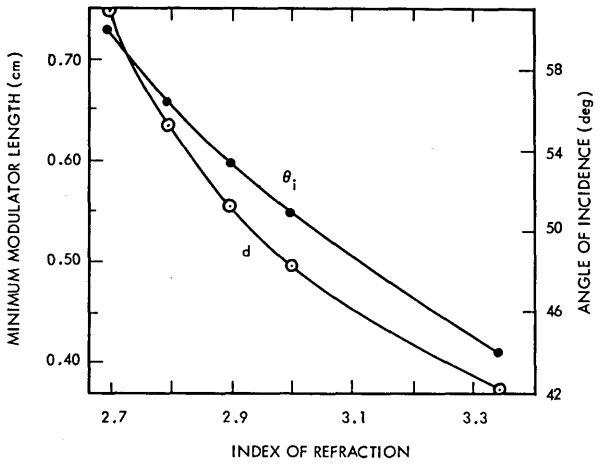

Fig. IX-7. Minimum modulator length and angle of incidence as functions of the index of refraction of the film.

index of the film. All analytical and numerical computations are carried out in the MACSYMA computer language.

D. REMOTE SENSING OF ICE THICKNESS WITH A RADIOMETER

California Institute of Technology (Contract 953524)

Jin-Au Kong

In this report we treat inhomogeneities in snow and ice by Rayleigh scattering. The scattering cross section is given by

$$\sigma_s = \frac{8\pi}{3}\left(\frac{\epsilon_s - \epsilon}{\epsilon_s + 2\epsilon}\right)^2 k^4 a^6, \tag{1}$$

where ϵ_s is the dielectric constant of the sphere, and a is the radius. Let the number

of scattering centers per unit volume be N. The loss factor that is due to scattering is $k_s'' = N\sigma_s/2$; the factor 2 is needed because the scattering cross section is calculated from Poynting's power. The fraction of the volume occupied by the scatterers is $P = 4\pi Na^3/3$. For closely packed spheres, N can be as large as $\sqrt{2}/8a^3$ corresponding to a sphere in a hexagonal volume. Thus the maximum fraction of scattering centers is approximately 74%. Furthermore, the sphere size must be smaller than 10% of a wavelength in order for the Rayleigh limit to hold. In terms of P, the effective loss factor is

$$k_s'' = 2Pk^4a^3\left(\frac{\epsilon_s - \epsilon}{\epsilon_s + 2\epsilon}\right)^2. \tag{2}$$

A penetration depth d_p is defined as

$$(k''+k_s'')\, d_p = 1, \tag{3}$$

where $k'' = \mathrm{Im}(k_o\sqrt{\epsilon'+i\epsilon''})$, and $\epsilon' + i\epsilon''$ is the complex dielectric constant.

A probing depth D_p may be defined from $e_2(D_p) - e_1 = \delta$, where δ is the radiometer sensitivity, e_1 is the emissivity in the absence of the bottom layer, and e_2 is the envelope of the emissivity for a two-layer medium. Under the assumption of small loss, D_p is calculated to be

$$D_p = -(\ln x)/2(k''+k_s''), \tag{4}$$

where

$$x = \frac{(1-R_{01}^2)(R_{01}^2+\delta)^{1/2} + \delta R_{01} + R_{01}^3 - R_{01}}{R_{12}(1-R_{01}^4+\delta R_{01}^2)}.$$

For ice with $\epsilon' = 3.2\,\epsilon_o$, $\epsilon'' = 0.0032\,\epsilon_o$, $\epsilon_s = \epsilon_o$, and p = 20%, the probing depth is plotted in Fig. IX-8 for a = 0 and a = 0.003m. In order to illustrate the scattering effects, we have used small values for ϵ'' and a large dielectric constant ($80\,\epsilon_o$) for the subsurface. Evidently scattering loss tends to decrease the probing depth of a radiometer.

Emissivity of a layer of ice with thickness d on water is calculated from

$$e \approx \frac{(1-A^2)(1-|R_{01}|^2)}{1 + A^2|R_{01}|^2}, \tag{5}$$

where $A = |R_{12}|\exp[-2(k''+k_s'')d]$, R_{12} is the reflection coefficient at the ice-water

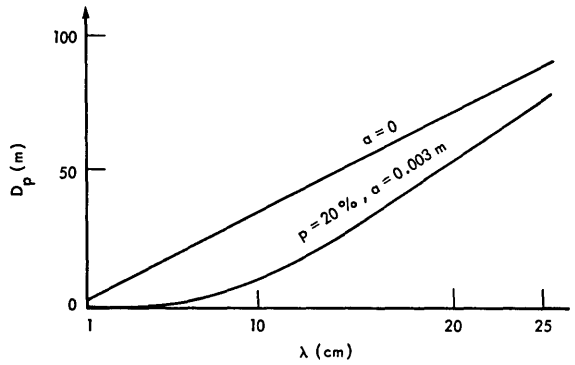

Fig. IX-8. Probing depth.

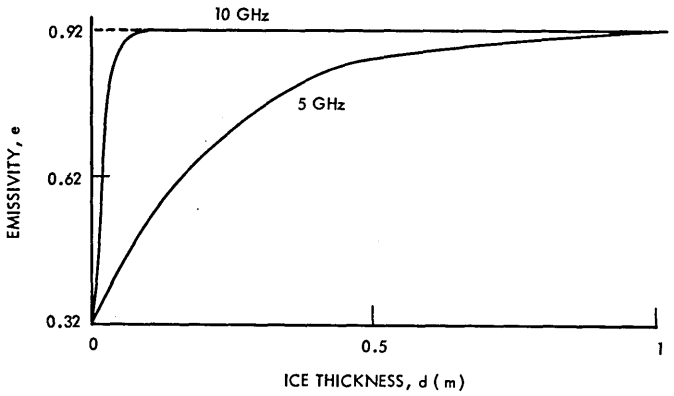

Fig. IX-9. Emissivity as a function of layer thickness d.

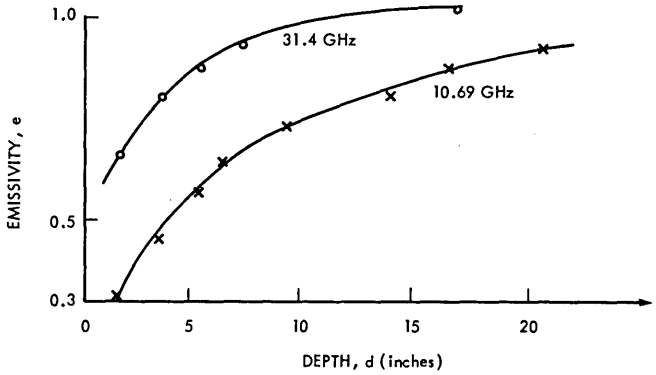

Fig. IX-10. Experimental results made in California Institute of Technology Jet Propulsion Laboratory model tank.

boundary, and R_{01} is the reflection coefficient at the air-ice boundary. In arriving at (5) we have neglected the oscillatory behavior of e because scattering renders the wave incoherent. The emissivity is plotted against ice thickness in Fig. IX-9.

In Fig. IX-10 some results are plotted from an experiment in the California Institute of Technology Jet Propulsion Laboratory model tank. The data were obtained with an aluminum plate in the tank covered with silica sand at depth d and observed with one radiometer at 31.4 GHz and another radiometer at 10.69 GHz.

E. MICROWAVE THERMAL EMISSION FROM CLOUDS

California Institute of Technology (Contract 953524)

Eni G. Njoku

A simple model for predicting the thermal microwave emission of a single cloud or rain layer in the atmosphere is proposed. The results will aid in the interpretation of remote sensing data from the earth's surface, taken under cloud-cover conditions.

The model is shown in Fig. IX-11 in which the emitting layer has vertical depth h,

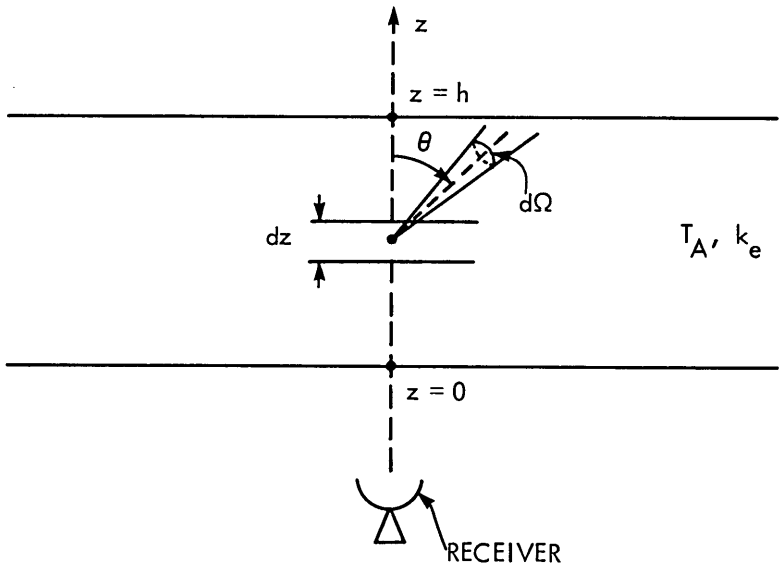

Fig. IX-11. Model geometry.

and is infinite in horizontal extent. Properties of the medium, such as temperature T_a and extinction coefficient k_e, are uniform with depth.

From radiative transfer theory, the received thermal radiation from the layer in terms of brightness temperature is

$$T_B = T_A(1-\bar{\omega})(1-e^{-\tau}) + \bar{\omega}\int_0^\tau J(\tau')\, e^{-\tau'}\, d\tau', \tag{1}$$

where

$\tau = k_e h$ ("optical depth" of layer)

$k_e = k_a + k_s$ (sum of absorption and scattering coefficients)

$\bar{\omega} = k_s/k_e$ (single-scattering albedo)

$J(\tau') = \int_{4\pi} T(\theta)\frac{P(\theta)}{4\pi}\, d\Omega$ (source of in-scattered radiation)

$T(\theta)$ = intensity of radiation scattered from direction θ

$P(\theta)$ = normalized phase function describing the scattering pattern.

At frequencies where scattering is unimportant $\bar{\omega} \to 0$, and we obtain

$$T_B = T_A(1-e^{-\tau}). \tag{2}$$

At higher frequencies where first-order scattering becomes important (higher orders of scattering neglected) $T(\theta)$ takes the form

$$T(\theta) = T_A(1-\bar{\omega})\left[1 - \exp\left\{-k_e\begin{pmatrix}h-z\\ -z\end{pmatrix}\Big/\cos\theta\right\}\right]; \quad \begin{pmatrix}0 \le \theta \le \pi/2\\ \pi/2 \le \theta \le \pi\end{pmatrix}. \tag{3}$$

Assume an isotropic phase function, then (1) can be integrated analytically to obtain

$$T_B = T_A(1-\bar{\omega})\left[(1-e^{-\tau}) + \frac{\bar{\omega}}{2}f(\tau)\right], \tag{4}$$

where $f(\tau) = (1-e^{-\tau})[1-e^{-\tau}+\tau E_1(\tau)] + \ln 2 - E_1(\tau) + E_1(2\tau) - e^{-\tau}[E_1(\tau)+\gamma+\ln\tau]$. For nonisotropic scattering, numerical integration of (1) is necessary.

The parameters k_e and $P(\theta)$ are obtained from the scattering by individual droplets, under the assumption that these droplets are spherical and of pure water. Assuming also that conditions within the medium are such that the scattering by individual droplets is incoherent, and using the drop-size distribution of Deirmendjian[1]

$$n(r) = Ar^\alpha \exp(-Br^\beta), \tag{5}$$

where A, B, α, β are constants, we obtain

$$\begin{aligned} k_e &= \int_0^\infty n(r)\, C_e(r)\, dr \\ P(\theta) &= \frac{1}{k_s}\int_0^\infty n(r)\, C_s(r)\, p(\theta, r)\, dr, \end{aligned} \tag{6}$$

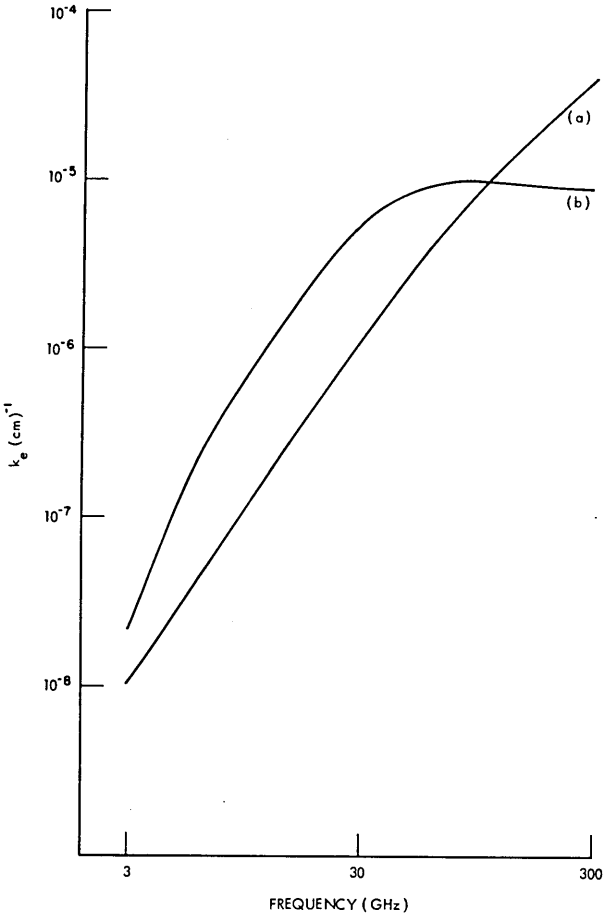

Fig. IX-12.

Extinction coefficients vs frequencies for models (a) and (b).

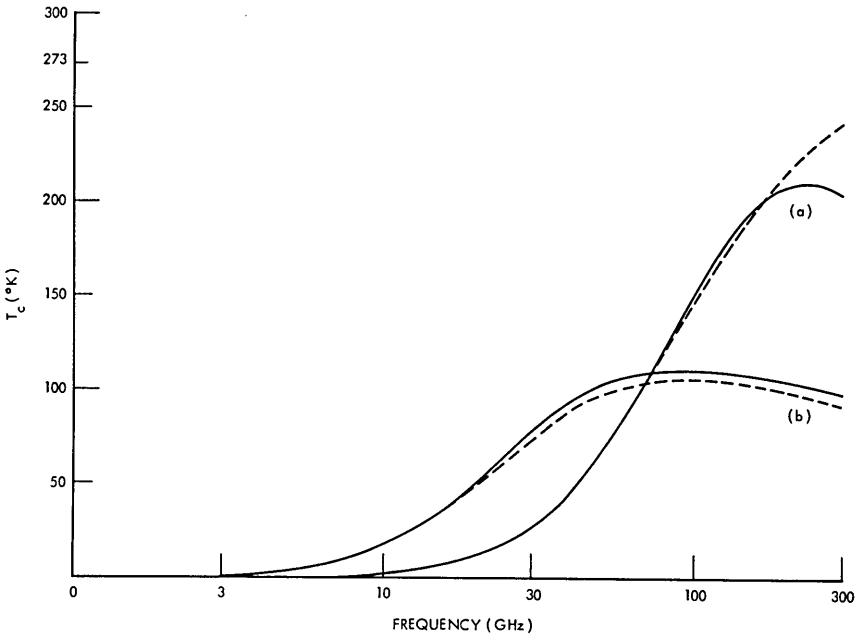

Fig. IX-13.

Brightness temperatures for models (a) and (b).

where $C_e(r)$, $C_s(r)$, and $p(\theta, r)$ are the extinction and scattering cross sections and phase function, respectively, for scattering by a single particle as given by Mie theory.[2]

Results computed by using a cloud and a rain model adapted from Gaut and Reifenstein[3] are as follows:

(a) Cumulus cloud $r_c = 20\ \mu$, $C_1 = 5.0$, $C_2 = 0.3$, $T_A = 273\,^\circ K$, $h = 1.0$ km

(b) Rain (12 mm/hr) $r_c = 400\ \mu$, $C_1 = 5.0$, $C_2 = 0.5$, $M = 0.5\ g/m^3$

where r_c is the mode radius of the drop distribution and M is the water content of the layer.

Figure IX-12 shows extinction coefficients vs frequency for the two models. Of interest are the saturation effects at $f \cong 95$ GHz (b), and $f > 300$ GHz ((a), not shown), as expected from the extinction cross sections of Mie theory. The models have equal water

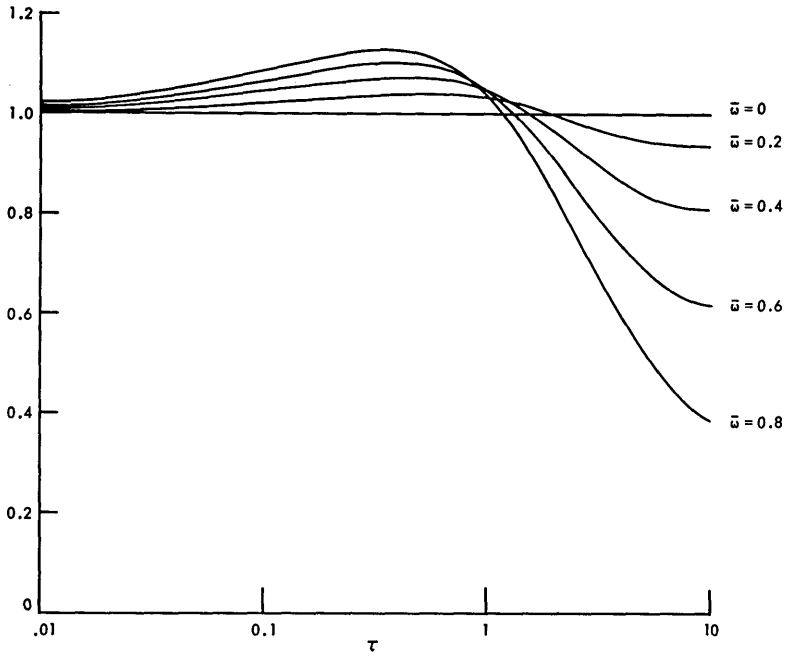

Fig. IX-14. Ratio of single-scattering to pure absorption emission.

content ($M = 0.5\ g/m^3$); for, although the droplets in (b) are much larger than those in (a) they are fewer in number. The dominance of these two effects interchanges at ~100 GHz crossover frequency.

Figure IX-13 shows the received brightness temperatures according to (4), for the two models. Also shown (dashed lines) is the result (2) in which the effects of scattering are neglected ($k_e = k_a$). Thus it is clear that first-order scattering becomes important at frequencies of 80 GHz for model (a) and 15 GHz for model (b). It is also evident that scattering can either increase or decrease the cloud brightness temperature, depending on the optical depth, τ, of the cloud. This can be seen by plotting the ratio of T_B in (4) to T_B in (2) (see Fig. IX-14). For large values of optical depth τ this ratio is always less than 1, since thermally emitted radiation scattered out of the line of sight reduces the amount of received radiation. Radiation is also scattered into the line of sight, thereby increasing the effective path length over which thermal emission can occur. This last factor becomes important as the optical depth decreases, and results in the crossover to ratios greater than 1, at a value of τ that depends on the single-scattering albedo ω.

References

1. D. Deirmendjian, Electromagnetic Scattering on Spherical Polydispersions (Elsevier, New York, 1969).

2. H. C. van de Hulst, Light Scattering by Small Particles (John Wiley and Sons, New York, 1957).

3. E. C. Reifenstein and N. E. Gaut, "Microwave Properties of Clouds in the Spectral Range 30-40 GHz," Technical Report No. 12, Environmental Research & Technology, Inc., Waltham, Massachusetts, 1971.